EREM 82/1
Journal of Environmental Research, Engineering and Management
Vol. 82 / No. 1 / 2026
pp. 100–118
10.5755/j01.erem.82.1.40088

Electro-chlorination using Titanium Alloy Electrodes with and without Coating and Formation of Trihalomethane during Water Disinfection

Received 2025/01 | Accepted after revisions 2025/12

https://doi.org/10.5755/j01.erem.82.1.40088

Electro-chlorination using Titanium Alloy Electrodes with and without Coating and Formation of Trihalomethane during Water Disinfection

Sapna R. Shinde[1], Sayali Apte[1*], Philipp Otter[2]

[1] Department of Civil Engineering, Symbiosis Institute of Technology, Symbiosis International University, India

[2] University of Kassel, Germany

***Corresponding author:** sayali.apte@sitpune.edu.in

The research investigates the in-situ chlorine generation potential and durability of graphite, titanium, newly identified Ti6Al4V, and coated Ti6Al4V electrodes under varying electric voltage, electrolysis time, inter-electrode distance, and electrolyte concentration, through experimental investigations using a solar-powered electro-chlorination (EC) lab-scale set-up. The experimental observations revealed that the maximum concentration of Chlorine Stock Solution (CSS) was achieved for the coated Ti6Al4V electrode (35.45 mg/L) under optimized conditions: 10 V electric potential, 60 min electrolysis time, 4 cm inter-electrode distance, and 4 g/L electrolyte concentration, for the developed laboratory set-up. The coated Ti6Al4V electrode outperforms both graphite and the Ti6Al4V electrode without coating in terms of electrode durability, indicating the effectiveness of the coated Ti6Al4V electrode in terms of maximum chlorine generation and durability. The CSS was used for water disinfection, and the quantum of trihalomethanes (THMs) generated was measured using gas chromatography–mass spectroscopy (GC-MS). It was observed that the THMs formed after disinfection using the EC-generated CSS are below the permissible limit for drinking water. The research concludes that the solar-powered EC set-up provides a safe, sustainable, and energy-efficient solution for water disinfection. The novel coated Ti6Al4V electrode exhibits effectiveness and durability during EC, with minimum THMs formation.

Keywords: chlorination, water disinfection, disinfection by products (DBPs), THMs, THMs minimization, electro-chlorination.

Introduction

The United Nations' Sustainable Development Goal (UN SDG) 6, part of the 2015 Sustainable Development Goals, aims to foster a sustainable future and ensure universal access to safe, potable drinking water by 2030. Despite of the global efforts to promote the consumption of potable water, remote rural areas continue to face the challenge of contaminated drinking water, resulting in waterborne diseases. The lack of infrastructure for drinking water treatment in rural and remote regions is primarily due to the high costs associated with centralized water treatment systems and its maintenance, making them financially unsuitable for low-income households. Consequently, the lack of access to safe, pathogen-free water leads to the increase in waterborne illnesses in rural households (Bain et al., 2019; Amrose et al, 2015). The problem can be addressed by decentralized and cost-effective water disinfection systems (Hossain et al., 2017; Shannon et al., 2008).

Water disinfection processes, such as chlorination, ultraviolet (UV) light, and ozone treatment, are most commonly used for combating these disease-causing pathogens. Among these methods, chlorination is most widely used due to its capacity to maintain residual effects in treated water (Hua et al., 2006; Kim et al., 2001; Chu et al., 2012). Although chlorination is efficient in removing the harmful pathogens, it also poses challenges concerning the storage, transport, and handling of chlorine (Ghernaout et al., 2019; Morris et al., 1992). Therefore, it is important to develop safe, decentralized, and economically viable treatment technologies for water disinfection in remote areas to address the health problems arising due to the consumption of contaminated drinking water. Literature indicates that decentralized systems offer benefits in promoting safe drinking water practices at reduced costs and maintenance requirements (Domenech, 2015; Jimenez-Moleon and Gomez-Albores, 2011).

Electro-chlorination (EC) is a promising decentralized treatment process for in-situ water disinfection. It is an electrochemical method in which the passage of an electric current through electrodes immersed in an electrolyte generates fresh chlorine in situ. While EC water disinfection offers a convenient and highly efficient means of producing pathogen-free water, its utilization has been limited by the unfamiliarity of the process (Kraft 2008). The effect of anode and cathode surface area, the intra-electrode distance, and the type of cathode and anode on EC is investigated in the literature (Khelifa et al., 2004; Ghalwa et al., 2012). Choi et al. (2013) investigated the design and operational constraints that affect the current efficiency and power consumption of an EC system. According to the literature, few investigations have been conducted into the effects of changes in electrolyte and inter-electrode distance (Choi et al., 2013). Saha and Gupta (2017) designed an EC model using graphite and stainless steel as anode and cathode, respectively (Saha and Gupta, 2017). The research involved only one type of electrolyte. Alexander Kraft (2008) reviewed the electrochemical process for water disinfection and concluded that EC is a convenient and highly efficient technique for producing pathogen-free water despite its unfamiliarity. Djamel et al., (2010) compared the chlorination and electrochemical process processes for water disinfection through multiple laboratory experiments and concluded that electro-chemical disinfection is more effective than chlorination. There are fewer studies on EC pilots and their utility for water disinfection in the literature. Otter et al. (2019) investigated the EC technique through a pilot installed at Kalyani, West Bengal, India. This pilot has a capacity of 2000 L/d and meets the local requirements by providing safe water to rural communities. From the literature, it can be inferred that further research is needed for exploring the efficient electrode combination for maximum production of in-situ chlorine with less corrosion improving the longevity of the EC electrode combination.

The formation of disinfection by-products (DBPs) is also a challenge in the water disinfection process. These are the by-products of the reaction between the disinfectant and naturally occurring Organic Matter (NOM) in water (Xiaoxiao et al., 2023). DBPs affect human health due to their carcinogenic properties (Health Canada, 2019), and controlling NOM and DBPs is challenging (Barrett et al., 2000).

DBPs are generated during nearly all water disinfection processes, like conventional chlorination, UV, ozonation, and EC (Liao et al., 2024; Chu et al., 2012). As a result of disinfection, based on the water characteristics and the type of NOM present in the water, a variety of DBPs are formed (Xiaoxiao et al., 2023). Liang and Singer (2003) is one of the few highest cited experimental works that studied the factors affecting the formation of DBPs. The literature concluded that aliphatic structured substitutes present in water are responsible for the maximum formation of trihalomethane DBP (Liao et al., 2024). The most widely used disinfectants

worldwide are sodium hypochlorite and chloramines, while the most commonly existing DBP after disinfection is trichloromethane (THMs) (Righi et al., 2012; Jalil et al., 2018). Literature illustrates that long-term exposure to the THMs may cause serious diseases like bladder cancer, rectal and colon cancer, and also affects the reproductive system (Smith, 2007; Villanueva et al., 2015; Evlampidou et al., 2020). Cao et al. (2016) investigated the relationship between blood markers of delayed conception associated with THMs in drinking water and embryonic growth and the gestational phase (Bond et al., 2011; Cao et al., 2016). The study's findings suggested increased parental exposure to THMs may significantly affect embryonic growth. Several factors influence the type and amount of DBP formation, including the type of disinfectant, concentration of disinfectant, contact time of disinfectant, type of precursors, and concentration of precursors (Liang and Singer, 2003). Valdivia-Garcia et al. (2019) conducted a comprehensive study analysing samples from 33 countries, covering over 50% of the global population, to determine the annual average concentrations of THMs. Results indicated that the highest levels of THMs from conventional chlorination are observed in Australia, followed by Cyprus, South Africa, Malta, and Ireland. Additionally, Valdivia-Garcia et al. (2019) suggested that increased mean temperatures, potentially attributed to global warming, could lead to the formation of elevated THMs. Under a mid-range scenario of a 1.8°C temperature rise, a projected 39% increase in THMs by 2050 was estimated (Valdivia-Garcia et al., 2019; Clayton et al., 2019). Notably, the maximum limit for THMs presence in drinking water is set at 80 µg/L, as stipulated by the Environmental Protection Agency (EPA) of the United States. Observation reveals that the quantity of THMs generated from conventional chlorination treatment often approaches or exceeds the EPA limit. Despite these findings, literature on THMs formation and EC remains scarce (Dubey et al., 2020). The author notes a lack of relevant literature indicating experimental detection of THMs following disinfection via EC treatment. Moreover, studies on developing safe, sustainable, and decentralized water disinfection systems are limited.

The primary objective of the present study was to investigate the effectiveness and durability of newly identified Ti6Al4V and coated Ti6Al4V electrode material to produce in-situ chlorine using EC through detailed experimentation using the developed solar-powered EC lab set-up. In addition, the study examined the disinfection efficiency and the quantum of THMs generation during water disinfection using the generated chlorine.

The detailed experimentation on the newly identified electrode material Ti6Al4V, with and without coating, for in-situ chlorine generation, as well as a detailed study on the quantification of THMs formation during the EC process, is the novelty of the present study.

Materials and Methods

Material

Graphite, titanium (Ti), Ti6Al4V, and Ti6Al4V with chromium nitride coating were the four electrode materials used as anodes and cathodes for the EC process in the present study. The electrodes were procured from a local vendor, and the chromium nitride coating on the Ti6Al4V electrode was performed using physical vapor deposition (PVD) methodology. The EC was performed using the same electrode material for both the anode and the cathode.

Graphite electrodes were preferred in electrolysis primarily due to their exceptional electrical conductivity. Graphite's unique structure allows many electrons to move freely between its atomic layers. This conductivity arises because graphite bonds utilize three of the four electron shells of a carbon atom, allowing the fourth electron to be free to move. As a result, these free electrons effectively facilitate the smooth progression of the electrolysis process. Furthermore, graphite electrodes offer an economical solution. Titanium electrodes have a relatively low electrical resistivity, making them efficient conductors of electricity during the electrolysis process. This characteristic enables the more effective transfer of electric current, facilitating the desired chemical transformations. Ti6Al4V, also known as Ti64, is an α + β titanium alloy with high strength, low density, high fracture toughness, excellent corrosion resistance, and superior biocompatibility. The Ti6Al4V electrode is henceforth referred to as the titanium alloy electrode or Ti alloy electrode. A chromium nitride coating was applied to the Ti alloy electrode to increase the corrosion resistance. Chromium nitride coating was used because it is resistant to chlorine attack, making it an ideal electrode for efficient EC. Out of the four electrodes investigated in the present study, the Ti alloy electrode, both with and without coating,

has not been used by researchers previously for EC.

The reason behind the selection of Ti and Ti alloy electrodes for EC was the reaction that Ti undergoes with atmospheric oxygen to form a fine layer of TiO_2, also known as titania, on the electrode through the oxidation process. Oxygen, with a higher electronegativity (3.5) compared to Ti (1.54), in the covalent bond between Ti and oxygen in the TiO_2 molecule, may cause a slight shift of the shared pair of electrons towards the oxygen, resulting in a partial positive charge on the Ti. This might contribute to the overall externally applied positive potential, attracting a higher quantum of opposite-charged chloride ions (Cl^-) and enhancing the bulk transfer of chlorine to the Ti electrode. In contrast, with a graphite electrode, Cl^- ions are attracted solely due to the charge generated by the external potential applied, as the electrode material possesses high electronegativity. Consequently, the migration of Cl^- ions is more pronounced with a Ti electrode than with a graphite electrode.

The laboratory-grade NaCl and KCl salts used for preparing electrolytes in this study were procured from Thermo-Fisher Scientific Pvt. Ltd. The required quantities of NaCl and KCl were dissolved in distilled water to produce the electrolyte solutions, thereby eliminating the impact of potential trace contaminants and their interference.

Methodology for in-situ chlorine production

One of the essential tasks for the experimental study was designing and implementing a laboratory-scale EC system tailored explicitly for the disinfection of potable water, which utilizes solar energy as its sole power source. The devised EC laboratory set-up holds the potential to serve as a decentralized solution, offering significant advantages in drinking water disinfection for rural regions and addressing a critical need for adequate water disinfection in such areas. The laboratory-scale reactor measuring 26 cm x 24 cm x 20.5 cm has been developed to produce an in-situ chlorine stock solution for experimental purposes. (*Fig. 1*).

The developed lab set-up was configured with the same material for both the anode and cathode. The electrical energy required to operate the experimental set-up was sourced exclusively from DC solar power (6V panels x 2), facilitated by a connection to the anode and cathode, as illustrated in *Fig. 1*. Comparative analyses assessed outcomes in NaCl and KCl electrolytic environments across four distinct electrodes: graphite, titanium (Ti), a Titanium alloy electrode, and a coated

Fig. 1. *EC lab scale model set up*

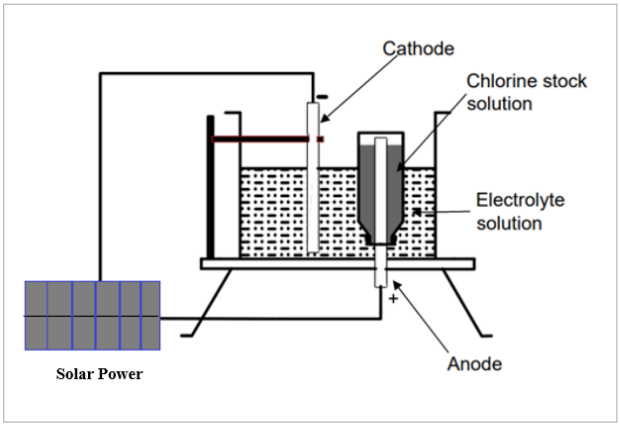

Titanium alloy electrode. The anode and cathode employed in this investigation were cylindrical, exhibiting dimensions of 30 cm in length and 1 cm in diameter.

The investigation compares in-situ chlorine production using graphite, Ti, Ti alloy, and coated Ti alloy electrodes in the developed laboratory set-up. A DC power was applied between the anode and cathode, resulting in the movement of anions and chlorine production (in the form of concentrated sodium hypochlorite solution) at the anode. The chlorine produced was collected using the liquid displacement method. The generated chlorine solution produced during the EC process at the anode was a concentrated solution of hypochlorite (OCl^-) ions and hypochlorous acid ($HOCl^-$), henceforth referred to as the Chlorine Stock Solution (CSS). This CSS was further used in the study to evaluate its effectiveness in disinfecting sample water.

The DPD titrimetric method was used to analyse the concentration of chlorine generated in the CSS after electrochemical treatment, as per the APHA Standard Methods 4500-Cl B, Iodometric Method (APHA). The experiments are performed in triplicate, and concordant or average values are reported to minimize the experimental errors. During the electrolysis of a sodium chloride (NaCl) solution, when an electrical potential is applied with inert electrodes, oxidation of Cl^- ions occurs at the anode, producing chlorine gas (Cl_2), and reduction of sodium ions (Na^+) takes place at the cathode, forming elemental sodium. Similarly, H_2O splits into oxygen gas (O_2) and hydrogen gas (H_2) during water electrolysis. Other reactions occur due to the presence of sodium hydroxide (NaOH) and hypochlorous acid ($HOCl^-$) in the electrolyte.

At the anode, electrolysis leads to the evolution of both chlorine and oxygen gases. However, due to the higher solubility of chlorine compared to oxygen, the generated CSS predominantly contains chlorine.

The various parameters considered for experimentation were determined based on preliminary trials. Following initial experimental trials and a review of existing literature, the voltage range was set from 2V to 20V in increments of 2V. It was observed that voltages exceeding 10V resulted in excessive electrode erosion.

Electrolysis time (ET) as varied from 15 minutes to 120 minutes with 15-minute increments after each experiment. Notably, constant chlorine production was observed from an ET of 60 minutes onwards, making the time variation up to 120 minutes sufficient for understanding further trends. After each experiment, the interelectrode distance was varied from 3 cm to 10 cm with 1 cm increments. It was observed that a decrease in chlorine concentration occurred after an inter-electrode distance of 5 cm.

The electrolyte concentration ranged from 0.5 g/L to 5 g/L, based on preliminary experiments, revealing that concentrations exceeding 4 g/L resulted in excessive electrode corrosion. All variations were conducted separately for sodium chloride and potassium chloride electrolytes for graphite, Ti, Ti alloy, and coated Ti alloy electrodes. While monitoring the effect of one parameter on chlorine formation, the other parameters were kept constant to avoid interference in the outcome results. The inspections for all parameter combinations taken during the experiments were graphically presented for graphite, Ti, Ti alloy, and coated Ti alloy electrodes using NaCl and KCl electrolytes.

The CSS produced through the electrochemical process was used for water disinfection. The required amount of chlorine dosage was determined to remove microbial contamination from the concentration of CSS (17.72 mg/L) generated during the EC process and the chlorine demand of the sample waters. For different chlorine dosages, the E. coli removal efficiency was experimentally determined before and after disinfection of the sample water. The compact dry plates produced by Hiserve Germany were used to detect E. coli in water samples before and after disinfection. E. coli for different chlorine dosages was studied to determine the exact chlorine dosage for maximum removal of E. coli.

Methodology for THMs detection

The THMs analysis was conducted using gas chromatography – mass spectroscopy (GC–MS) with an Agilent GC 7890B and MSD 5977B (single quadrupole) instrument. Following the APHA 5240D method, one µL of the sample was injected in split-less mode using an auto-liquid sampler. HP-5 (30 m × 0.25 mm), a column with helium as the carrier gas at a flow rate of 1 mL/min, was used. The inlet and transfer line temperatures were set to 250°C and 300°C, respectively. The GC oven was initially set at 40°C, held for 1 minute, then increased to 90°C at a rate of 10°C/min, and

Fig. 2. *Calibration curve for known Concentration of THMs and corresponding Peak Area*

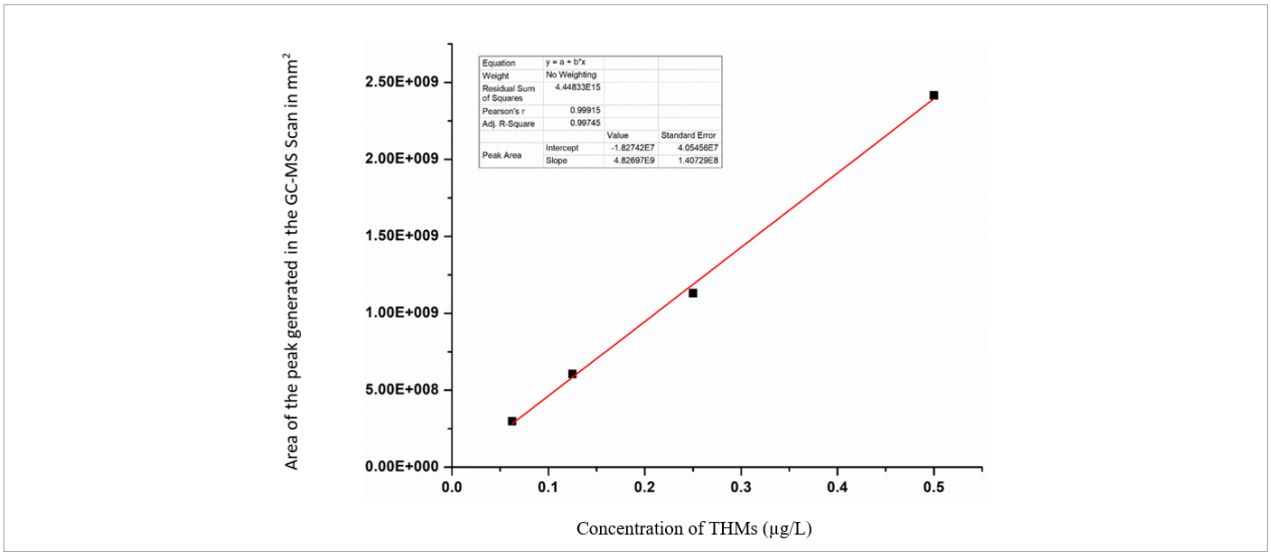

subsequently increased to 250°C at a rate of 15°C/min, with a 2-minute hold. The MS source temperature was 250°C, the quadrupole temperature was 200°C, with a solvent delay of 2 minutes, and the mass range was 30 to 600 m/z. The chlorine dosage was added to the water sample with a contact time of 30 min. The samples were prepared using a liquid-liquid extraction process, and the organic solvent at the bottom was collected using a syringe needle and transferred to the injection port of a gas chromatograph for analysis. The GC–MS provides the peaks for the formation of THMs. The method used for quantification of the THMs based on the GC–MS results is as follows. A reference/ calibration curve was plotted for known concentrations versus peak area for THMs obtained by GC-MS. This curve was used as a reference to determine the THMs concentration of the unknown samples through linear fittings, and the actual concentration of generated THMs was evaluated (*Fig. 2*).

Experimentation plan

The experimental plan used for the present study is shown in *Fig. 3*. For objective 1, the lab scale EC set up developed for production of chlorine was optimized for maximum generation of chlorine concentration by considering varying parameters like electric voltage (2–12V), EC Time (ET) (15–20 min), interelectrode distance (3–10 cm), concentration of electrolytes (0.5–5 g/L), type of electrolytes (NaCl / KCl). *Fig. 3* also mentions the number of experiments performed for system optimization and selection of the superior electrode. Each experiment was performed in triplicate to minimize experimental and human error. For each electrode pair, such as Graphite, Ti, Ti alloy, and coated Ti alloy, 108 experiments were performed (36 x 3), totalling 432 experiments per electrolyte. Experiments were performed separately for NaCl and KCl electrolytes. Experimental analysis was conducted for all these variations across all electrodes under varying parameters to achieve maximum chlorine generation. As the life of the electrode was crucial in the EC process, the longevity of the electrodes was determined to assess the life of the electrode.

The same CSS generated from the EC lab scale model was used for the disinfection of water samples. The microbial characteristics were analysed before and after disinfection of the sample waters for various chlorine dosages. The THMs, which were predominantly found in DBPs in the sample water after the disinfection treatment, were detected and quantified using gas chromatography for various chlorine dosages. From the experimental data, the optimum chlorine dosage required for maximum removal of E. coli and minimum formation of THMs was determined. *Fig. 3* explains the detailed methodology of the present research study.

Results and Discussions

Experimentation to optimize the EC lab set up for maximum chlorine generation by Voltage Variation

The graphite, titanium, Ti alloy, and coated Ti alloy electrodes were used separately in the electro-chlorination process, with the same electrode material used for both anode and cathode. The voltage was varied from 2 V to 10 V with a 2 V rise. Other parameters were kept constant, including 60 minutes of ET, a 5 cm interelectrode distance, and an electrolyte strength of 0.5 g/L. From the experimentation, it was observed that the highest CSS concentration was detected for the coated Ti alloy electrode using a NaCl electrolyte at 10 V. The electric voltage trend for all types of electrodes was the same, irrespective of the type of electrolyte. The CSS concentration, even when the voltage was increased beyond 10V, remains almost constant. The highest CSS concentration achieved for the coated Ti alloy electrode, at 10 V electric voltage, 60 minutes of ET, 5 cm inter-electrode distance, for electrolyte strength of 0.5 g/L, was 17.72 mg/L using NaCl electrolyte and 12.40 mg/L using KCl electrolyte (*Fig. 4a* and *4b*) From the experiments it was observed that the CSS concentration generated using NaCl electrolyte was more compared to KCl electrolyte.

Efficiency in chlorine production depends on Faraday's Law of Efficiency (FE), which is the ratio of the actual chlorine produced to the theoretical maximum. High FE relates to efficient electron transfer for chlorine generation. This study revealed that titanium electrodes achieved a higher FE compared to graphite, indicating they minimize unwanted side reactions. Therefore, for on-site chlorine production, titanium electrodes are a superior choice due to their superior FE, maximizing chlorine output. During the electrolysis process, simultaneous non-Faradic reactions occur alongside the Faradic reactions, which involve oxidation-reduction

Fig. 3. *Methodology adopted for Optimum Parameter setting for efficiency*

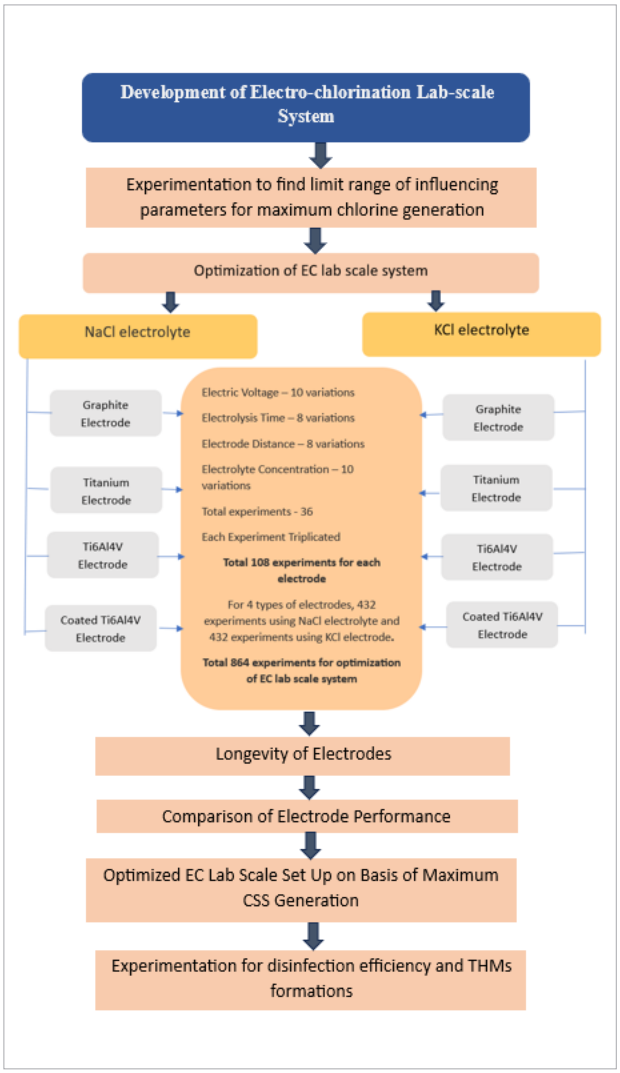

processes. The non-Faradic reactions at the electrode contribute to the formation of an electric double layer. This phenomenon may hinder the migration of Cl^- ions towards the anode, resulting in a potential limitation in chlorine production at the anode. Therefore, the development of this electric double layer may explain the sustained chlorine production even with an increase in electric voltage beyond 10 V. This insight contributes to a deeper understanding of the complex electrochemical processes at play during electrolysis.

Effect of variation in ET on chlorine generation

The ET was varied from 15 min to 120 min for all types of electrodes, with other parameters kept constant: electric voltage of 10 V, an interelectrode distance of 5 cm, and an electrolyte concentration of 0.5 g/L. The experiments revealed that the maximum in-situ chlorine was generated at 60 minutes of ET for all electrodes, irrespective of the electrolyte used, but the concentration of CSS varied. Subsequent increases in ET resulted in a slight decrease in chlorine generation. The maximum CSS concentration recorded was 17.72 mg/L (NaCl electrolyte) and 12.40 mg/L (KCl electrolyte) using the coated Ti alloy electrode at the 60-minute mark (*Fig. 5a* and *5b*). For the above observations, the ET was finalized at 60 minutes for subsequent experiments. The decrease in the CSS concentration after 60 minutes of ET may be due to the observed formation of a double layer (Garcia-Lopez et al. 2024) at the electrodes after 60 minutes of electrolysis, which restricts the further movement of chlorine ions toward the anode, ultimately leading to a marginal reduction or a plateau in chlorine concentration after 60 minutes of ET. This

Fig. 4 (a). *CSS concentration using respective electrodes for varying voltage using NaCl electrolyte*

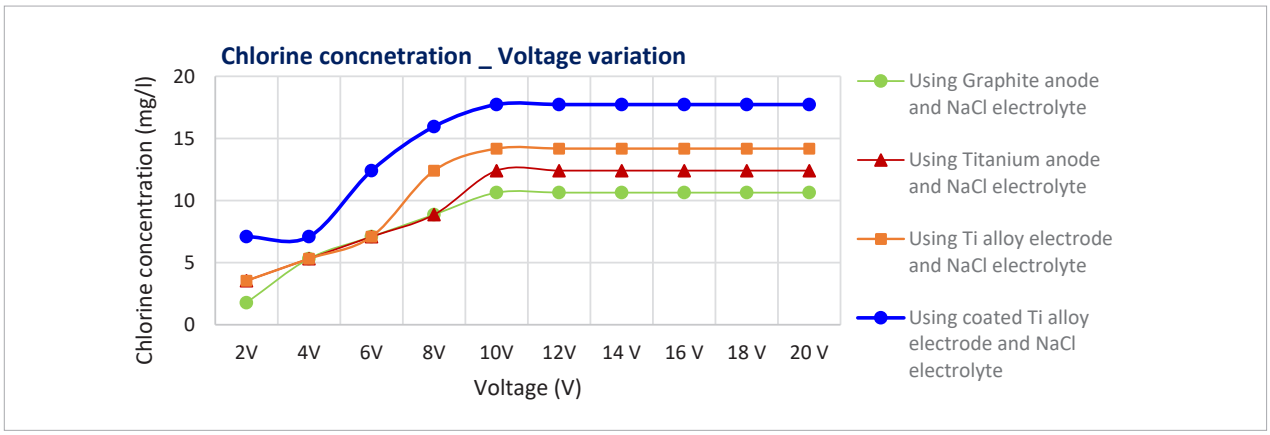

phenomenon suggests that a similar process may be occurring in the ongoing experimentation, explaining the absence of a significant increase in chlorine generation beyond the 60-minute electrolysis duration.

Fig. 4 (b). *CSS concentration using respective electrodes for varying voltage using a KCl electrolyte*

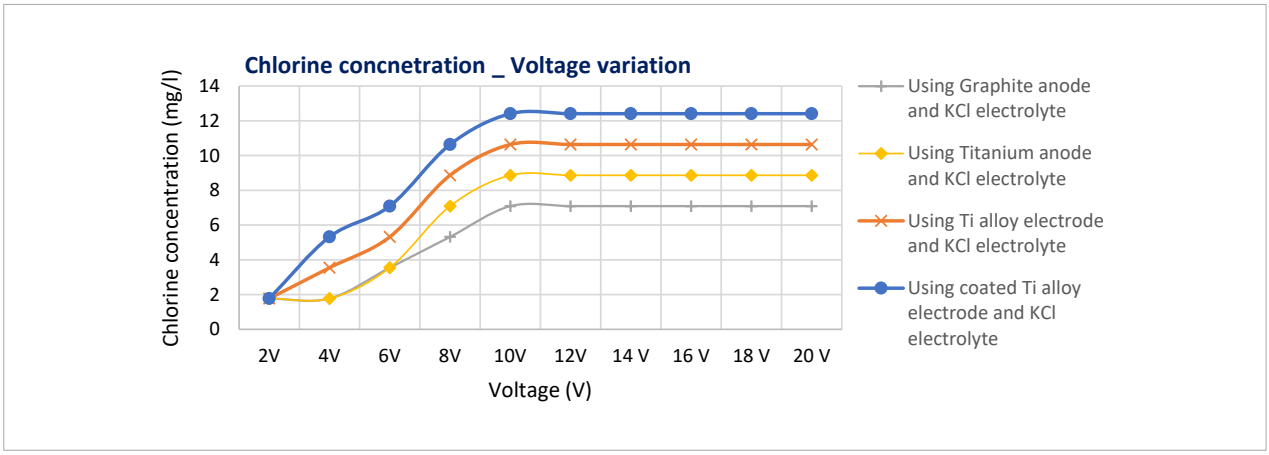

Fig. 5 (a). *CSS concentration by varying the ET using NaCl electrolyte for respective electrodes*

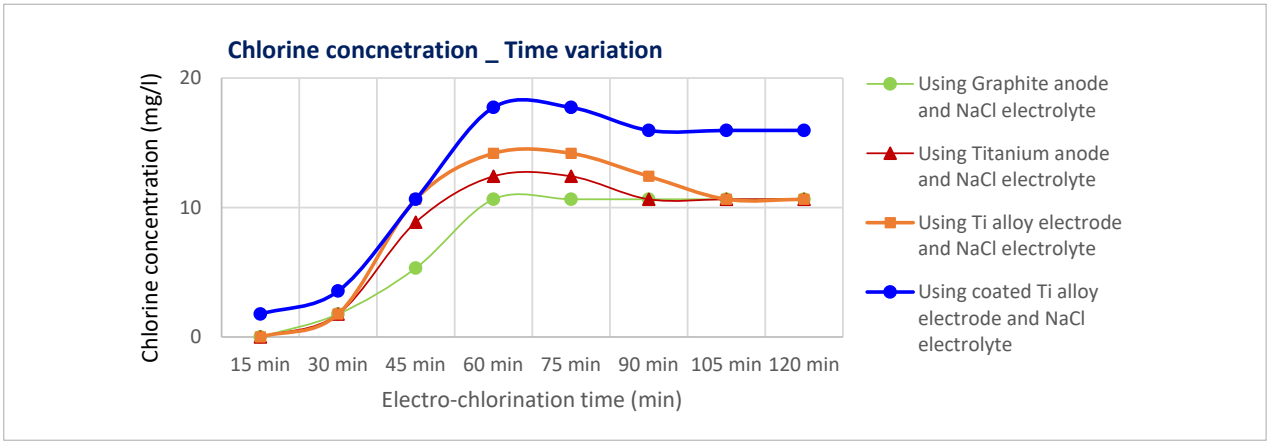

Fig. 5 (b). *CSS concentration by varying ET using a KCl electrolyte for respective electrodes.*

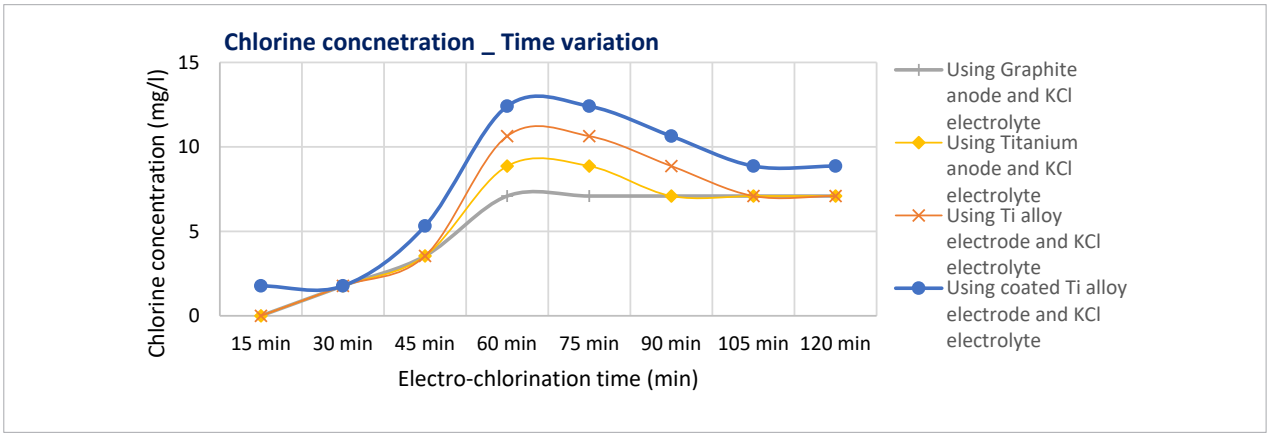

Effect of variation in inter-electrode distance on chlorine generation

The inter-electrode distance also affects chlorine generation; therefore, studies were conducted over a range of 3 cm to 10 cm with an increment of 1 cm. From the experiments, it was observed that at a 4 cm inter-electrode distance, the solution generates a maximum CSS concentration for each respective electrode. The maximum concentration of CSS was obtained at an inter-electrode distance of 4 cm and 5 cm, while a decrease in CSS concentration was observed beyond 5 cm, as shown in *Fig. 6a* and *6b*. At a 10 cm inter-electrode distance, minimal chlorine generation was obtained for all types of electrodes and electrolytes. Therefore, further experiments were conducted at an inter-electrode distance of 4 cm.

Migration of charges was a crucial factor influencing chlorine generation during electrolysis, requiring a minimal inter-electrode gap for the movement of opposite charges towards the charged electrodes. This can be the reason for reduced CSS concentration observed at shorter inter-electrode distances. Conversely, at high inter-electrode distances, the electrolysis process was hindered due to the reduced intensity of the internal current, resulting in a decrease in ion migration. This inefficiency at greater interelectrode distances contributes to a less effective electrolysis process.

Fig. 6 (a). *CSS concentration generated by varying the electrode distance using NaCl electrolyte for respective electrodes*

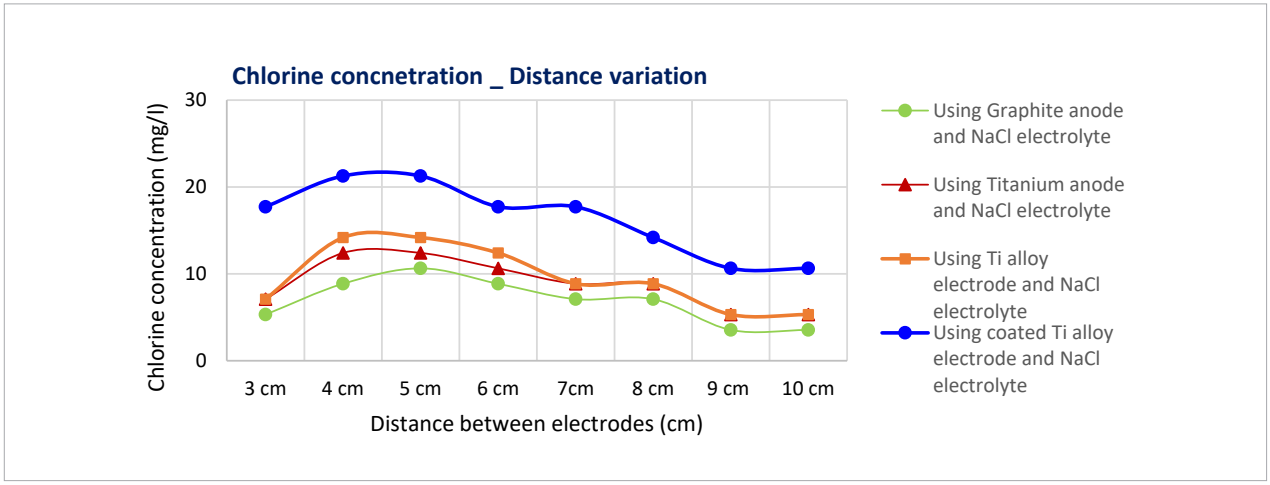

Fig. 6 (b). *CSS concentration generated by varying the electrode distance using a KCl electrolyte for the respective electrodes*

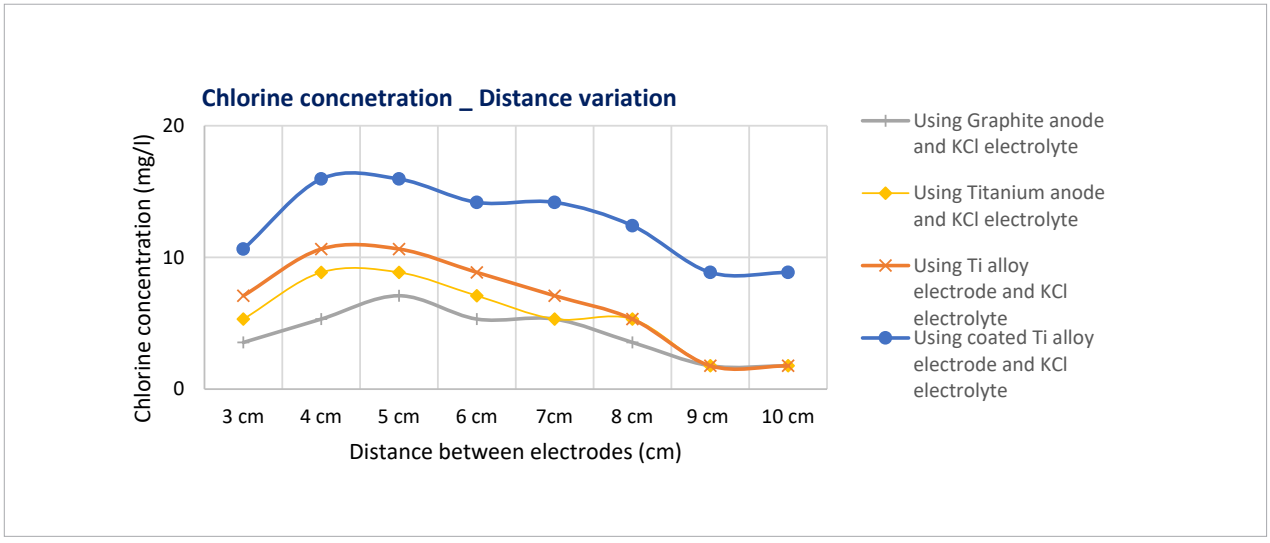

Fig. 7 (a). *Variation in CSS concentration for varying electrolyte concentration using NaCl electrolyte for respective electrodes*

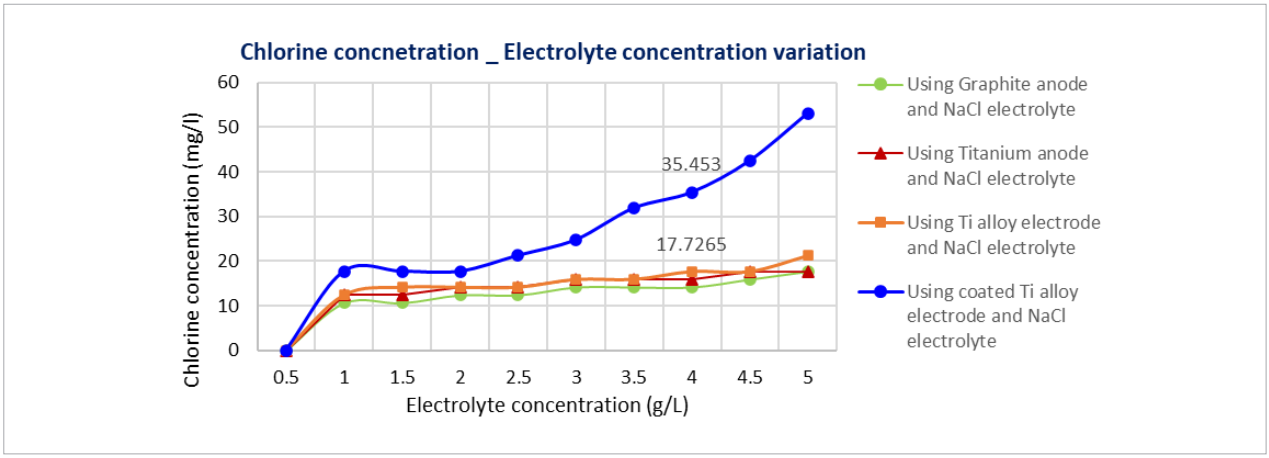

Fig. 7 (b). *Variation in CSS concentration for varying electrolyte concentration using KCl electrolyte for respective electrodes*

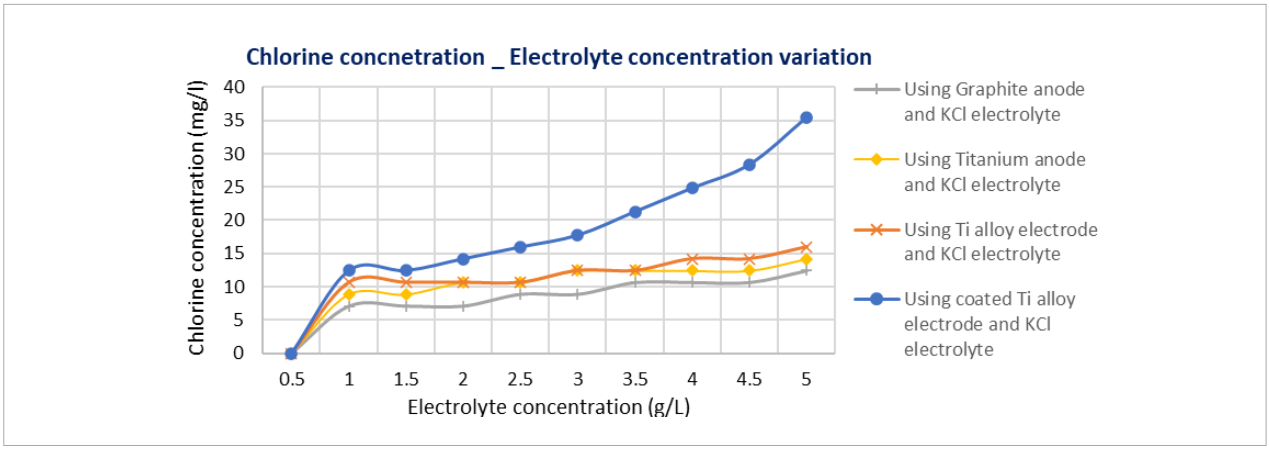

Effect of variation in electrolyte concentration on chlorine generation

The electrolyte concentration was varied from 0.5 g/L to 5 g/L to understand the effect of electrolyte concentration on the generated CSS concentration for all the types of electrodes. While studying the effect of electrolyte concentration, the other parameters were kept constant, such as an electric voltage of 10 V for 60 min ET and a 4 cm inter-electrode gap. From the study, it can be concluded that the increase in CSS concentration was proportional to the electrolyte concentration. However, the optimized electrolyte concentration was finalized at 4 g/L because electrode erosion increases after the electrolyte concentration exceeds 4 g/L, although the CSS concentration increases. The maximum CSS concentration obtained at 4g/L for the coated Ti alloy electrode was 35.45 mg/l using NaCl electrolyte and 24.81 mg/L using KCl electrolyte (*Fig. 7a and 7 b*). The CSS concentration obtained using NaCl electrolyte was higher compared to KCl electrolyte.

The optimized conditions for achieving maximum chlorine generation were identified as 10 V electric voltage, 60 minutes of ET, a 4 cm interelectrode distance, and a 4 g/L electrolyte concentration (*Fig. 7a*).

During the EC process, both faradic and non-faradic reactions occur, resulting in the generation of a diffuse layer between the electrodes. At lower ion concentrations, the increased thickness of the diffuse layer hampers the movement of ions towards the anode. Consequently, chlorine generation at lower electrolyte concentrations was less efficient compared to higher concentrations (Brown et al., 2016).

Fig. 8. *Rate of material loss during the electro-chlorination process for the graphite electrode*

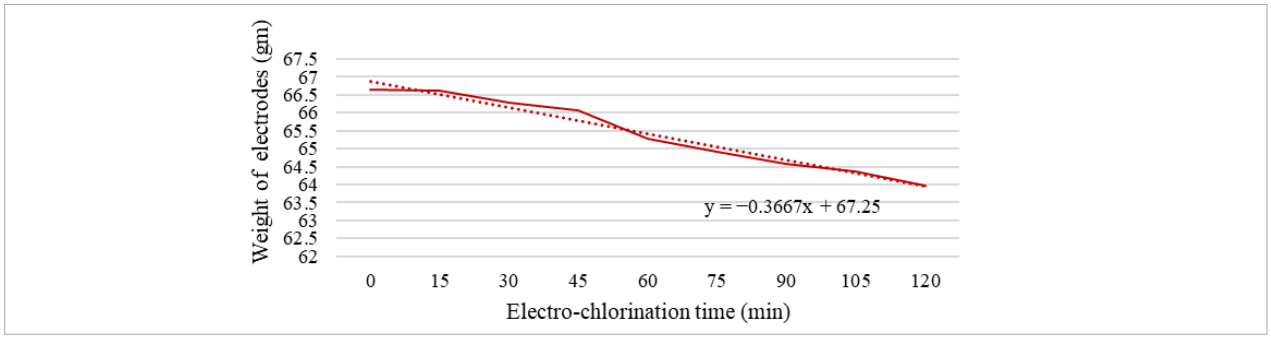

Fig. 9. *Rate of material loss during the electro-chlorination process for the Ti electrode*

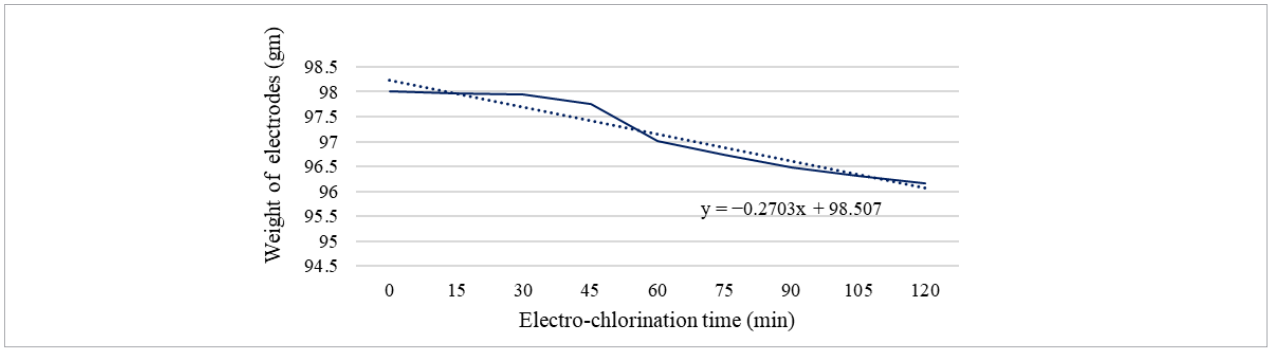

Fig. 10. *Rate of material loss during the electro-chlorination process for the Ti alloy electrode*

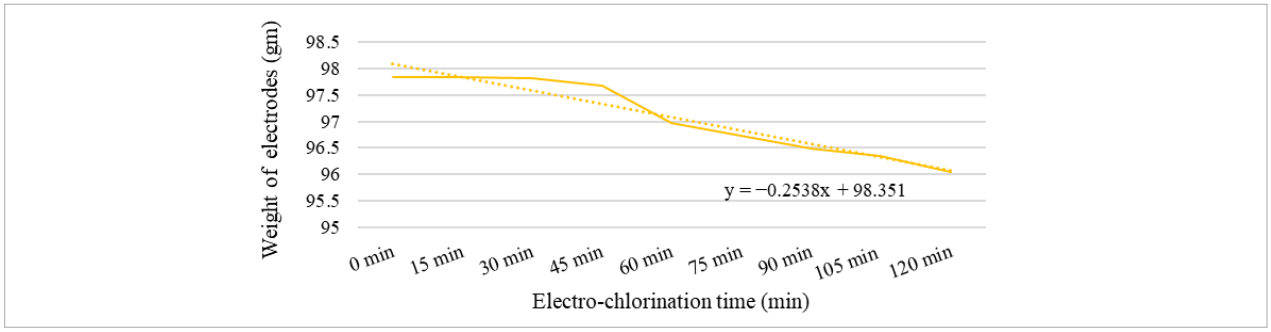

Fig. 11. *Rate of material loss during the electro-chlorination process for coated Ti alloy electrode*

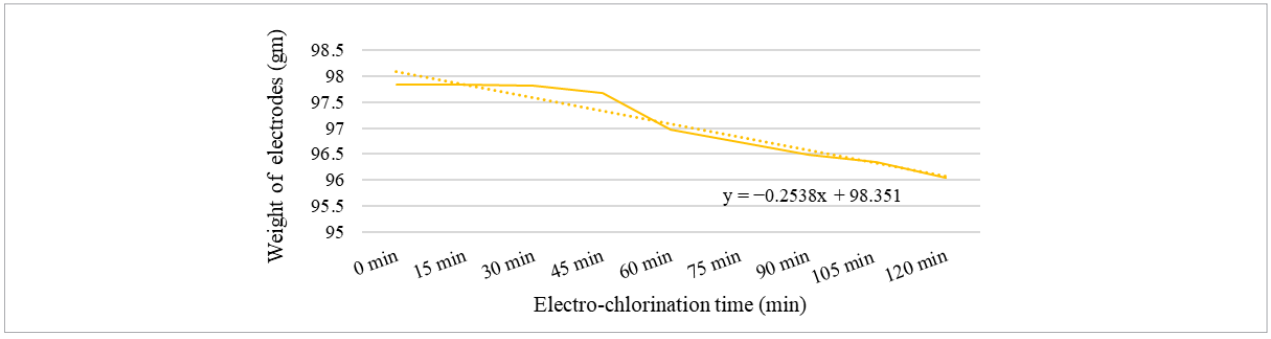

The solar power required to generate maximum chlorine for an optimized lab-scale set-up was 16×10^{-3} kW/hr. The system operates entirely on solar energy, yielding significant economic benefits. The integration of solar power effectively reduces dependence on conventional electricity sources, resulting in substantial energy and cost savings and making it suitable for usage in rural and remote areas.

During the electrolysis process, the anode experiences erosion, a phenomenon acknowledged by prior research, including the work of Khelifa et al. (2004), which highlighted electrode crumbling and erosion as notable drawbacks in continuous electrocoagulation processes. This study explicitly investigates the longevity of electrodes using a NaCl electrolyte. To assess the electrode's resilience over prolonged electrolysis durations, the weight loss of graphite, Ti, Ti alloy, and coated Ti alloy electrodes was quantified through erosion measurements. The (*Fig. 8*, *9*, *10*, and 11) depict the remaining weight of the electrodes throughout continuous EC, revealing a nearly linear correlation between the loss of electrode weight and the ET.

In the context of the current investigation, the observed rate of material loss for the graphite electrode was approximately 0.024 gm/min. Similarly, the material loss for the Ti electrode was found as 0.0153 gm/min, while for the Ti alloy electrode, it measured 0.0149 gm/min, and the material loss for the coated Ti alloy electrode was 0.00875 (gm/min). These findings contribute valuable insights into the erosion dynamics of different electrodes over varying durations of continuous electro-chlorination, offering essential considerations for the practical application of this electrochemical process.

From *Fig. 8*, *9*, *10*, and *11*, it was inferred that the loss in graphite and Ti electrode was more than that of the coated Ti alloy and coated Ti electrode as the ET increased. Ti alloy electrodes, being resistant to erosion by nature, exhibited less erosion compared to other electrodes. The coated Ti electrode had the minimum material loss compared to all the electrodes under consideration, due to the chromium nitride coating, which was resistant to chlorine attack, making it an ideal electrode for efficient electro-chlorination.

Based on the above observations of CSS concentration under optimized conditions and the experimental observations on material loss of the electrode during the EC process, the three electrodes were also compared for techno-economic feasibility. From the comparison, it can be concluded that the quantum and concentration of CSS that can be produced over the lifetime of a pair of electrodes are maximum for the coated Ti alloy electrode compared to graphite, Ti, and Ti6Al4V electrodes of the exact dimensions (*Table 1*).

Table 1. *Comparison between graphite, Ti, Ti6Al4V, and coated Ti6Al4V electrode*

Sr no	Electrode material	Cost of the electrode (for volume 23.565 cubic cm)	Material weight for given volume	Concentration of CSS (mg/L) *	Total quantity of chlorine in 230 ml of stock solution *(mg)	Rate of material loss during electro-chlorination (gm/min) *
1	Graphite	144	66.66	14.18	3.2614	0.02
2	Ti	700	98	15.95	3.6685	0.02
3	Ti6Al4V	700	97.84	17.72	4.0756	0.01
4	Coated Ti6Al4V	825	97.85	35.45	8.1535	0.00875

** For optimized conditions*

Comparison between the performance of electrodes and electrolytes

The maximum concentration of CSS generated under optimized conditions (10 V electric voltage, 60 minutes of ET, a 4 cm interelectrode distance, and a 4 g/L electrolyte concentration) for graphite, titanium, Ti alloy, and coated Ti alloy electrodes was compared for NaCl and KCl electrolytes. *Fig. 12* compares the maximum CSS concentration generated by various electrodes under optimized conditions.

From the results, it was observed that the maximum chlorine generation was achieved using a NaCl electrolyte for each type of electrode. Therefore, NaCl was considered an efficient electrolyte compared to KCl for maximum chlorine generation in the EC process. The maximum CSS concentration of 35.45 mg/L was obtained using a NaCl electrolyte and a coated Ti alloy electrode. The measured concentration of dissolved titanium (Ti) is significantly below a level of concern. This is supported by regulatory toxicology, as the U.S. EPA has not established a maximum

Fig. 12. *Comparison of the maximum CSS concentration generated for respective types of electrodes for both NaCl and KCl electrolytes*

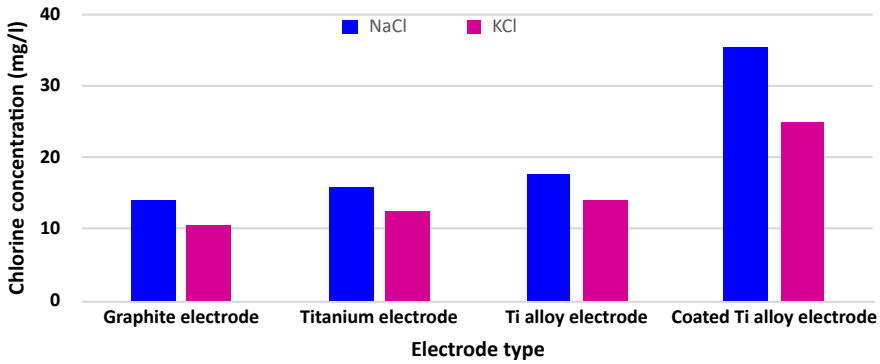

contaminant level (MCL) for titanium in drinking water due to its chemical inertness and low systemic toxicity via the oral route (EPA, 2009; WHO, 1999). Furthermore, the WHO/FAO JECFA previously found TiO_2 to be non-toxic upon ingestion, noting its low absorption and lack of tissue accumulation (JECFA, 1970; EPA, 2009; WHO, 1999).

The NaCl ions were fully dissociated into solution as cations and anions, which conduct a strong electric current through the solution compared to the KCl electrolyte. Hence, results using the NaCl electrolyte might be better than those using the KCl electrolyte.

THMs generation during the disinfection process using the chlorine stock solution generatedusing EC

The efficacy of the CSS for disinfection of water was examined for samples with varying characteristics, especially NOM. The chlorine demand of the water sample tested was 0.3 (mg/l). The fresh CSS produced through the EC process was used for disinfecting the water sample. Subsequently, a bacteriological examination was conducted on the sample both before and after the disinfection process to check the efficacy of microbial removal.

According to the chlorine demand of the sample (0.3 mg/L) and the concentration of CSS (17.72 mg/L), a varying quantity of CSS was added separately into beakers containing the sample, as shown in *Fig. 14*. To understand the impact of hypo-chlorination, breakpoint chlorination, and hyperchlorination on the disinfection efficiency and DBP formation, the CSS was added for dose less than the chlorine demand (0.15 mg/L, 0.23 mg/L), equal to chlorine demand (0.3 mg/L) and greater than chlorine demand (0.32 mg/L, 0.35 mg/L and 0.38 mg/L) to the sample separately in different containers. *Fig. 13* illustrates the chlorine dosages added to the sample, as explained in *Table 2*. The chlorine dosage and the quantity of CSS added are given in *Table 2*. From the detailed observations provided in *Table 3*, it was inferred that the CSS generated during the EC process was effective in water disinfection.

Fig. 13. *Different chlorine dosages were added to the water sample*

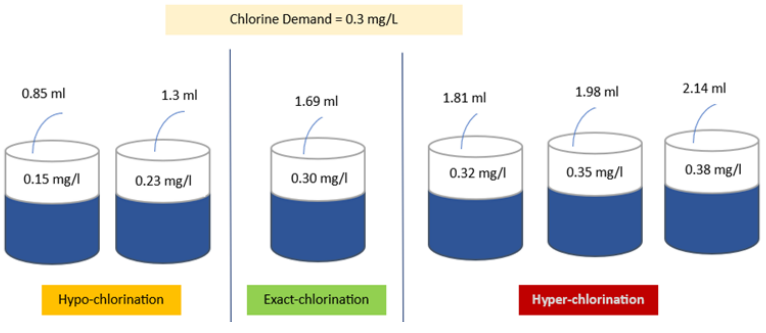

Table 2. *Chlorine dosage applied to the water sample*

Sr No.	Chlorination	Chlorine dosage variation mg/L	CSS (mL)
1.	Hypo-chlorination	0.15	0.85
2.	Hypo-chlorination	0.23	1.3
3.	Exact chlorination	0.3	1.69
4.	Hyper-chlorination	0.32	1.81
5.	Hyper-chlorination	0.35	1.98
6.	Hyper-chlorination	0.38	2.14

Fig. 14. *Type of THMs*

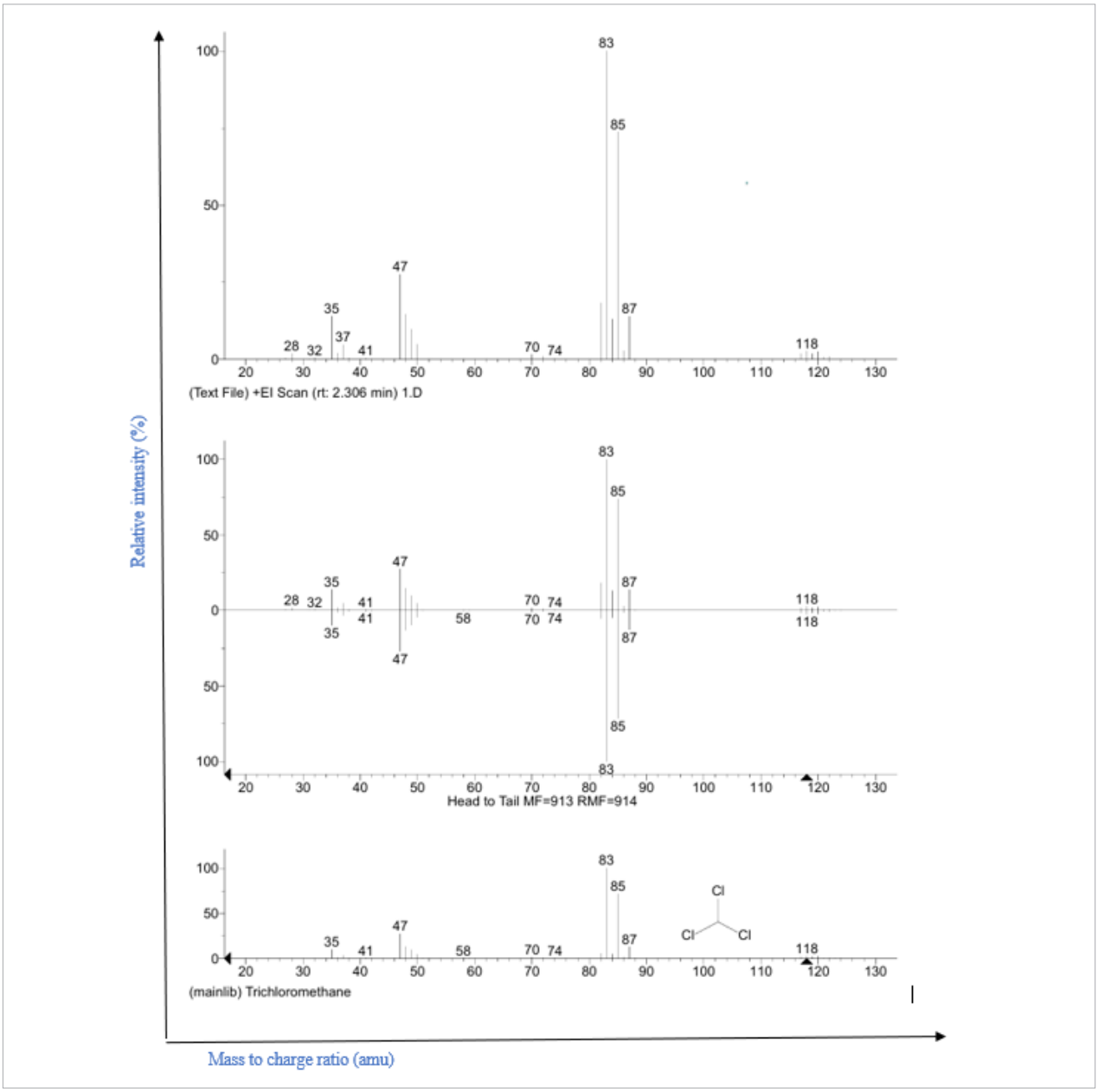

Table 3. *E. coli removal efficiency from the sample water and DBP formation for different chlorine dosages*

Sr No	Chlorination	Chlorine dosage (mg/L)	E. coli before disinfection CFU/100 ml	E. coli after disinfection CFU/100 ml	E-Coli Removal Efficiency (%)	THMs Area on curve mm^2	THMs unit µg/L
1	Hypo-chlorination	0.15	196	184	61.22	6735539.04	0.00139
2		0.23	196	179	86.73	9434076.50	0.00195
3	Exact-chlorination	0.30	196	0	100	12354331.04	0.00254
4	Hyper-chlorination	0.32	196	0	100	48198092.81	0.00997
5		0.35	196	0	100	72596713.73	0.01501
6		0.38	196	0	100	88435442.11	0.01825

The disinfected sample was analysed for the type and quantity of DBPs generated using GC-MS. *Fig. 14* shows the types of DBPs generated, with THMs being the predominant DBP produced during the process.

The general maximum limit for THMs in drinking water was 80 µg/L as per environmental protection agency, United States (EPA)). Long-term exposure to DBPs above the permissible limit can lead to serious health effects.

The disinfected water sample with different chlorine dosages was analyzed for THM detection using GC-MS, as discussed in the methodology section.

For the water sample, the various chlorine dosages added to the sample water were 0.15 mg/L, 0.23 mg/L, 0.30 mg/L, 0.32 mg/L, 0.35 mg/L, and 0.38 mg/L, and were analyzed separately to detect the quantity and type of THMs formed (*Fig. 14*). The quantity of THMs generated was analyzed from the graphs generated by the GC and MSD detectors, shown below in *Fig. 16*. The X-axis represents the retention time, and the Y-axis represents the peak intensity of the product formed.

The data analysis reveals that THMs produced for chlorine dosages below the required amount of chlorine, i.e., 0.30 mg/L for the water sample, were lower. For higher chlorine dosages above the required dosage, the quantity of THMs formed was observed to be greater (*Fig. 15*) (*Table 3*).

From the retention time, the type of THMs was detected using a mass spectrometer detector. The details are as shown in *Fig. 14*. The *Fig.* consists of a main graph and a mirror-matched graph, where the type of compound detected is displayed along with its structure. From the analysis of all graphs, it was observed that the type of THMs detected in all the samples was the same, and it was trichloromethane; only the quantity of the THM compound differed for different chlorine dosages.

The increased chlorine dosage beyond the chlorine demand leads to an increase in the THMs production after breakpoint chlorination. Therefore, accurately determining the exact amount of chlorine dosage is crucial for achieving maximum E. coli removal and minimizing the generation of THMs.

Conclusion

The present paper discusses a detailed experimental investigation of the electro-chlorination (EC) process using a developed lab-scale solar-powered sustainable EC system for graphite, titanium, novel Ti6Al4V, and novel Ti6Al4V electrodes coated with chromium nitride. The study also investigates the type and quantity of DBPs formed during the disinfection by EC process. The detailed analysis revealed that for the developed EC model, under optimized conditions of a 10 V electric voltage, 60 minutes of electro-chlorination time, 4 cm electrode spacing, and a 4 g/L electrolyte concentration, a single pair of coated Ti6Al4V electrodes yield a maximum chlorine stock solution concentration of 35.45 mg/l as compared to graphite (14.18 mg/L), Ti (15.95 mg/L) and Ti6Al4V (17.72 mg/L) electrodes. However, it was worth noting that the longevity of the coated Ti6Al4V electrode was better compared to graphite, Ti, and Ti alloy electrodes during EC. The study concluded that the coated Ti6AL4V electrode stands out as one of the most effective electrodes for achieving maximum chlorine generation with minimal crumbling. The chlorine stock solution generated was found

to be effective in disinfecting sample water samples. Additionally, detailed experimentation was conducted to understand the disinfection by-products formed during the disinfection of water using the generated stock solution from the EC process for various samples.

The trihalomethanes (THMS) were detected as the prominent DBPs formed after disinfection of the water sample, and the quantity of THMs generated after EC disinfection for the sample was 0.00254 µg/L The study concludes that the coated Ti6Al4V electrode material is an efficient and durable material for the EC process. The experimental observations also indicate that the EC process is effective in minimizing the formation of THMs in disinfected water. This developed solar-powered EC set-up has the potential to serve as a decentralized solution, offering significant benefits for water purification in rural areas where effective disinfection is urgently needed.

Fig. 15. *THMs detection using gas chromatography for a water sample with different chlorine dosages, like (15a) 0.15 mg/L, (15b) 0.23 mg/L, (15c) 0.30 mg/L, (15d) 0.32 mg/L, (15e) 0.35 mg/L, (15f) 0.38 mg/L*

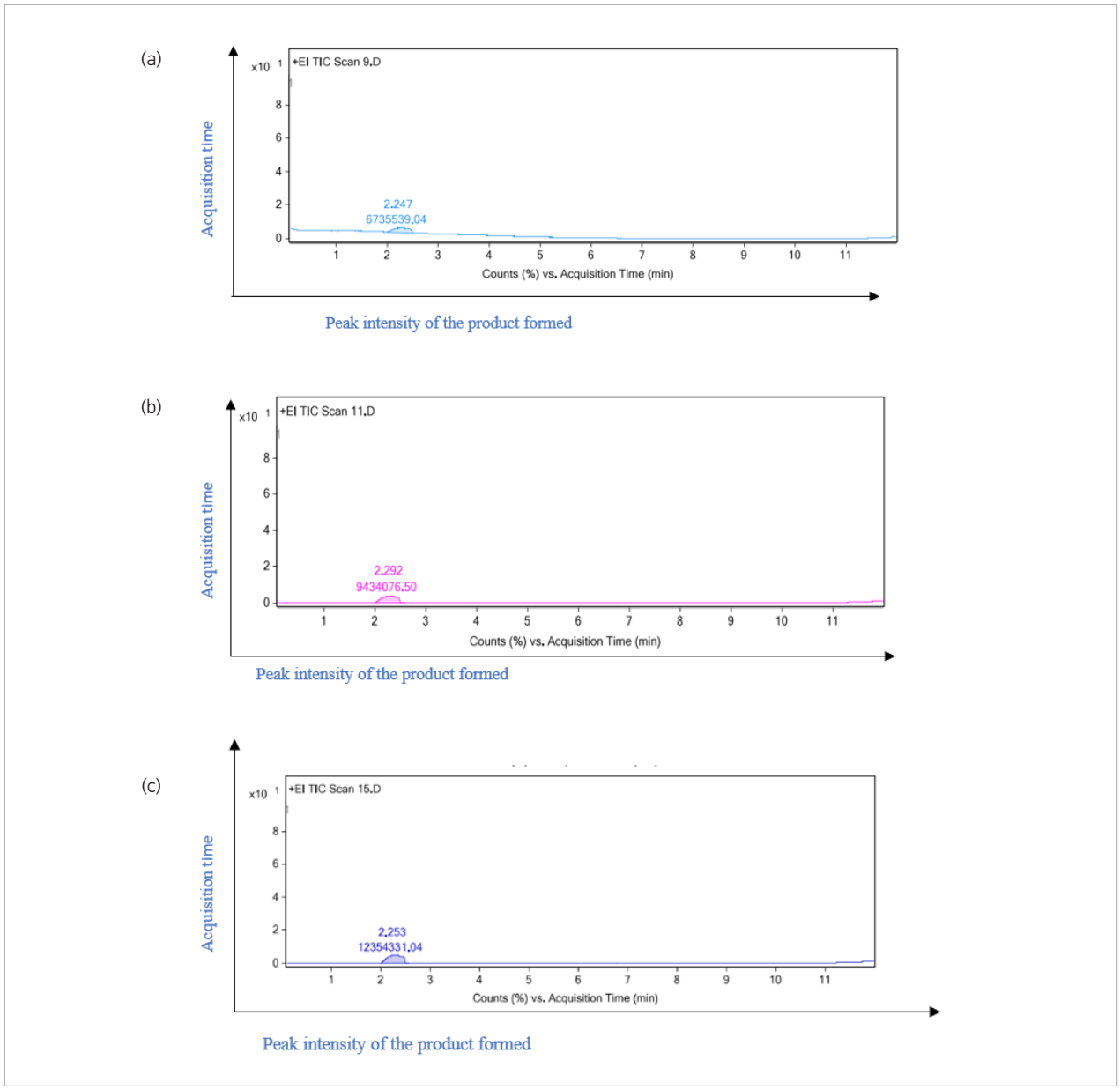

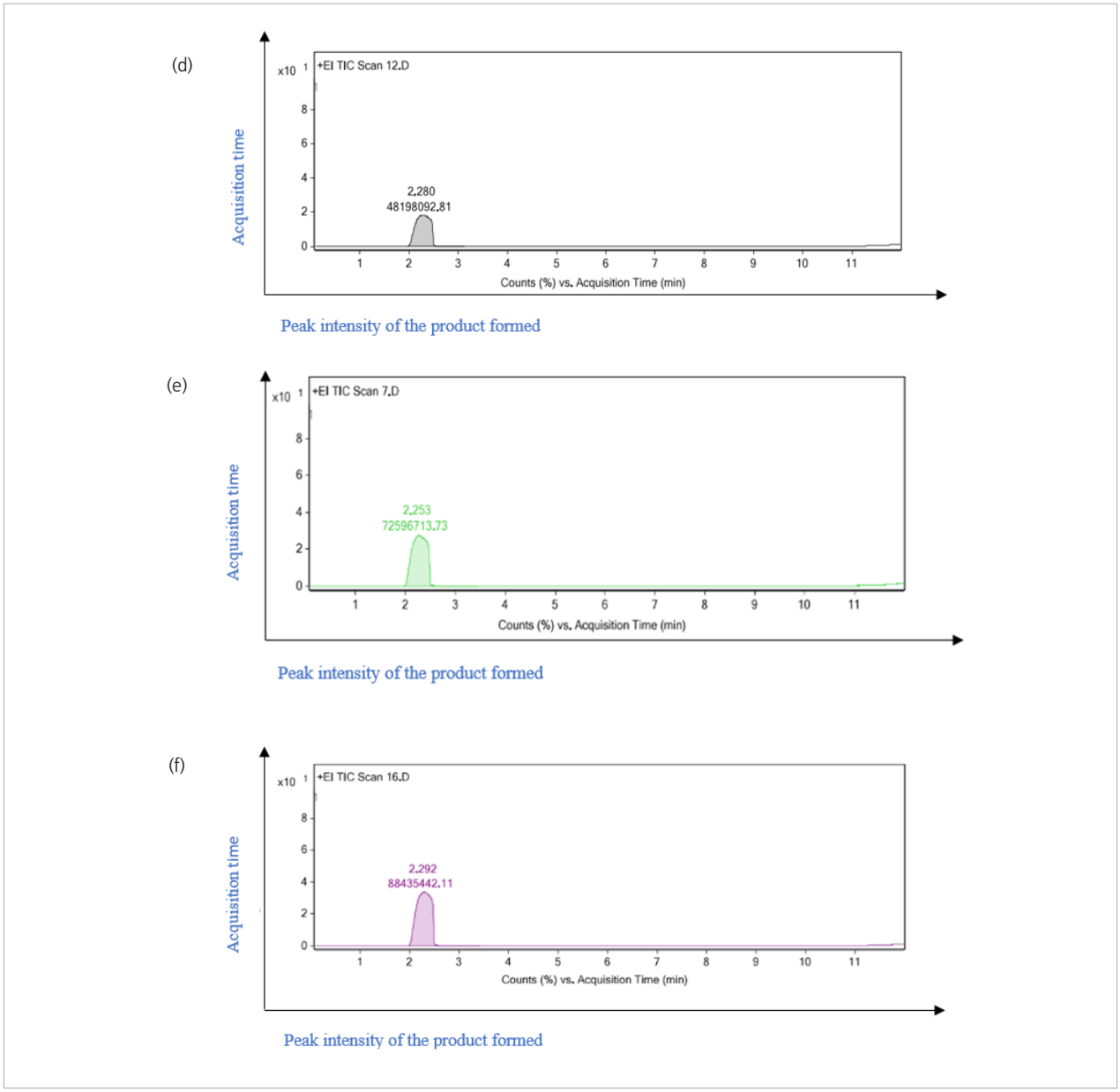

References

Amrose S., Burt Z., Ray I. (2015) Safe Drinking Water for Low Income Regions. Annual Review of Environment and Resources 40(1): 203–231. Available at: https://doi.org/10.1146/annurev-environ-031411-091819

Bain R., Cronk R., Wright J., Yang H., Slaymaker T., Bartram J., Hunter P. R. (2019) Fecal Contamination of Drinking Water in Low- and Middle-Income Countries: A Systematic Review and Meta Analysis Introduction. PLOS Medicine 16(1). Available at: https://doi.org/10.1371/journal.pmed.1001644

Barrett S. E., Krasner S. W., Amy G. L. (2000) Natural Organic Matter and Disinfection by Products: Characterization and Control in Drinking Water an Overview. ACS Symposium Series 761(11): 2–14. Available at: https://doi.org/10.1021/bk-2000-0761.ch001

Bond T., Goslan E. H., Parsons S. A., Jefferson B. (2011) Treatment of Disinfection by Product Precursors. Environmental Technology 32(1): 1–25. Available at: https://doi.org/10.1080/09593330.2010.495138

Brown M. A., Goel A., Abbas Z. (2016) Effect of Electrolyte Concentration on the Stern Layer Thickness at a Charged Interface. Angewandte Chemie International Edition 55(11): 3790–3794. Available at: https://doi.org/10.1002/anie.201512025

Cao W. C., Zeng Q., Luo Y., Chen H. X., Miao D. Y., Li L., Cheng Y. H., Li M., Wang F., You L., Wang Y. X., Yang P., Lu W. Q. (2016) Blood Biomarkers of Late Pregnancy Exposure to Trihalomethanes in Drinking Water and Fetal Growth Measures and Gestational Age in a Chinese Cohort. Environmental Health Perspectives 124(4): 536–541. Available at: https://pubmed.ncbi.nlm.nih.gov/26340795/

Choi J., Shim S., Yoon J. (2013) Design and Operating Parameters Affecting an Electro-chlorination System. Journal of Industrial and Engineering Chemistry 19(1): 215–219. Available at: https://doi.org/10.1016/j.jiec.2012.08.004

Chu W., Gao N., Krasner S. W., Templeton M. R., Yin D. (2012) Formation of Halogenated C-, N-DBPs from Chloramination and UV Irradiation of Tyrosine in Drinking Water. Environmental Pollution 161: 8-14. Available at: https://doi.org/10.1016/j.envpol.2011.09.037

Clayton G. E., Thorn R. M. S., Reynolds D. M. (2019) Comparison of Trihalomethane Formation Using Chlorine-Based Disinfectants Within a Model System Applications Within Point-of-Use Drinking Water Treatment. Frontiers in Environmental Science 7:35. Available at: https://doi.org/10.3389/fenvs.2019.00035

Domenech L. (2015) Rethinking Water Management: From Centralised to Decentralised Water Supply and Sanitation Models. December. Available at: https://raco.cat/index.php/DocumentsAnalisi/article/view/244658

Dubey S., Gusain D., Sharma Y. C., Bux F. (2020) The Occurrence of Various Types of Disinfectant By-Products (Trihalomethanes, Haloacetic Acids, Haloacetonitrile) in Drinking Water. In M. N. V. Prasad (Ed.), *Disinfection by-products in drinking water* (pp. 371–391). Butterworth-Heinemann. Available at: https://doi.org/10.1016/b978-0-08-102977-0.00016-0

EPA (U.S. Environmental Protection Agency) (2009) Titanium Dioxide: Inert Ingredients in Pesticide Products [or FQPA Reassessment]. Office of Pesticide Programs, Washington, DC.

Evlampidou I., Font-Ribera L., Rojas-Rueda D., Gracia-Lavedan E., Costet N., Pearce N., Vineis P., Jaakkola J. J. K., Delloye F., Makris K. C., Stephanou E. G., Kargaki S., Kozisek F., Sigsgaard T., Hansen B., Schullehner J., Nahkur R., Galey C., Zwiener C., Vargha M., Righi E., Aggazzottu G., Kalnina G., Grazuleviciene R., Polanska K., Gubkova D., Bitenc K., Goslan E. H., Kogevinas M., Villanueva C. M. (2020) Trihalomethanes in Drinking Water and Bladder Cancer Burden in the European Union. Environmental Health Perspectives 128(1): 1–14. Available at: https://doi.org/10.1289/EHP4495

Garcia-Lopez I., Arenas L. F., Hereijgers J., Águeda V. I., Garrido-Escudero A. (2024) Drinking Water Electro-chlorination in a Single-Pass Biomimetic Flow Cell with Zero Salt Dosing. ACS Sustainable Chemistry and Engineering 12(8): 3130–3141. Available at: https://doi.org/10.1021/acssuschemeng.3c07066

Ghalwa N.A., Tamos H., ElAskalni M., El Agha A.R. (2012) Generation of Sodium Hypochlorite (NaOCl) from Sodium Chloride Solution Using C/PbO2 and Pb/PbO2 Electrodes. International Journal of Minerals, Metallurgy and Materials 19(6): 561–566. Available at: https://doi.org/10.1007/s12613-012-0596-0

Ghernaout D., Alghamdi A., Ghernaout B. (2019) Microorganisms' Killing: Chemical Disinfection vs. Electro-disinfection. Applied Engineering 3(1): 13–19. Available at: https://doi.org/10.11648/j.ae.20190301.12

Health Canada (2019) Guidance on Natural Organic Matter in Drinking Water - Canada.ca. Government of Canada, 73. Available at: https://www.canada.ca/en/health-canada/programs/consultation-organic-matter-drinking-water/document.html#a1 (accessed 1 December 2024).

Hossain M. J., Kabir A. H. M. E., Jahan S. (2017) Safe Drinking Water Scarcity in the Southwestern Coastal Region of Bangladesh: A Scenario of Sarankhola Upazila, Bagerhat District. 6th International Conference on Water and Flood Management, 2017. Available at: https://www.researchgate.net/publication/320411224_safe_drinking_water_scarcity_in_the_southwestern_coastal_region_of_bangladesh_a_scenario_of_sarankhola_upazila_bagerhat_district

Hua W., Bennett E. R., Letcher R. J. (2006) Ozone Treatment and the Depletion of Detectable Pharmaceuticals and Atrazine Herbicide in Drinking Water Sourced from the Upper Detroit River, Ontario, Canada. Water Research 40(12): 2259–2266. Available at: https://doi.org/10.1016/j.watres.2006.04.033

Jalil A. M. F., Hamidin N., Nagoor Gunny A. A., Kamarudzaman A. N. (2018) Identification of Trihalomethanes (THMs) Levels in Water Supply: A Case Study in Perlis, Malaysia. E3S Web of Conferences 34. Available at: https://doi.org/10.1051/e3sconf/20183402043

JECFA (Joint FAO/WHO Expert Committee on Food Additives) (1970) Evaluation of Certain Food Additives and Contaminants. Eighteenth Report of the Joint FAO/WHO Expert Committee on Food Additives, Titanium Dioxide. WHO Technical Report Series No. 462.

Jimenez-Moleon M. C., Gomez-Albores M. A. (2011) Waterborne Diseases in the State of Mexico, Mexico (2000–2005). Journal of Water and Health 9(1): 200–207. Available at: https://doi.org/10.2166/wh.2010.149

Khelifa A., Moulay S., Hannane F., Benslimene S., Hecini M. (2004) Application of an Experimental Design Method to Study the Performance of Electrochlorination Cells. Desalination 160(1): 91-98. Available at: https://doi.org/10.1016/S0011-9164(04)90021-5

Kim K., Hong W., Lee K. (2001) Disinfection Characteristics of Waterborne Pathogenic Protozoa Giardia lamblia. 95–99. Available at: https://doi.org/10.1007/BF02931953

Kraft A. (2008) Electrochemical Water Disinfection: A Short Review. Platinum Metals Review 52(3): 177–185. Available at: https://doi.org/10.1595/147106708X329273

Liang L., Singer P.C. (2003) Factors Influencing the Formation and Relative Distribution of Haloacetic Acids and Trihalomethanes in Drinking Water. Environmental Science and Technology 37(13): 2920–2928. Available at: https://doi.org/10.1021/es026230q

Liao Y., Ji W., Wang Z., Tian Y., Peng J., Li W., Pan Y., Li A. (2024) Effects of Alternative Disinfection Methods on the Characteristics of Effluent Organic Matter and the Formation of Disinfection By-Products. Environmental Pollution 340: 122796. Available at: https://doi.org/10.1016/j.envpol.2023.122796

Morris R.D., Audet A.M., Angelillo I.F., Chalmers T.C., Mosteller F. (1992) Chlorination, Chlorination By-products, and Cancer: A Meta-analysis. American Journal of Public Health 82(7): 955–963. Available at: https://doi.org/10.2105/AJPH.82.7.955

Otter P., Malakar P., Sandhu C., Grischek T., Sharma S. K., Kimothi P. C., Nüske G.,Wagner M., Goldmaier A., Benz F. (2019) Combination of River Bank Filtration and Solar-driven Electro-Chlorination Assuring Safe Drinking Water Supply for River Bound Communities in India. Water 11: 122. Available at: https://doi.org/10.3390/w11010122

Righi E., Bechtold P., Tortorici D., Lauriola P., Calzolari E., Astolfi G., Nieuwenhuijsen M. J., Fantuzzi G., Aggazzotti G. (2012) Trihalomethanes, Chlorite, Chlorate in Drinking Water and Risk of Congenital Anomalies: A Population-Based Case-Control Study in Northern Italy. Environmental Research 116: 66–73. Available at: https://doi.org/10.1016/j.envres.2012.04.014

Saha J., Gupta S. K. (2017) A Novel Electro-chlorinator Using Low-Cost Graphite Electrode for Drinking Water Disinfection. Ionics 23: 1903–1913. Available at: https://doi.org/10.1007/s11581-017-2022-0

Shannon M., Bohn P., Elimelech M., Georgiadis J. G., Marias B. J., Mayes A. M. (2008) Science and technology for water purification in the coming decades. Nature 452: 301–310. Available at: https://doi.org/10.1038/nature06599

Smith M. (2007) Health Effects of Disinfection By-Products in Australian Drinking Waters. International Journal of Water 3(4): 347–355. Available at: https://doi.org/10.1504/IJW.2007.016318

Valdivia-Garcia M., Weir P., Graham D. W., Werner D. (2019) Predicted Impact of Climate Change on Trihalomethanes Formation in Drinking Water Treatment. Scientific Reports 9: 9967. Available at: https://www.nature.com/articles/s41598-019-46238-0

Villanueva C. M., Cordier S., Font-Ribera L., Salas L. A., Levallois P. (2015) Overview of Disinfection By-products and Associated Health Effects. Current Environmental Health Reports 2: 107–115. Available at: https://doi.org/10.1007/s40572-014-0032-x

WHO (World Health Organization) (1999) International Programme on Chemical Safety, Environmental Health Criteria 24. Titanium. World Health Organization.

Xiaoxiao L., Xie Z., Sun Y., Qiu J., Yang X. (2023) Recent Progress in Identification of Water Disinfection By-Products and Opportunities for Future Research. Environmental Pollution 337: 122601. Available at: https://doi.org/10.1016/j.envpol.2023.122601